Progress in Organic Coatings 154 (2021) 106189

Contents lists available at ScienceDirect

Progress in Organic Coatings

journal homepage: www.elsevier.com/locate/porgcoat

Short communication

# Highly conjugated visible and near-infrared light photoinitiating systems for radical and cationic polymerizations

Ali Suerkan, Investigation [a], Ecem Aydan Alkan, Investigation [b], Kerem Kaya, Visualization [a], Yasemin Arslan Udum [c], Levent Toppare [b,d,e,f,**], Yusuf Yagci [a,g,*]

[a] Department of Chemistry, Istanbul Technical University, Maslak, Istanbul, 34469, Turkey
[b] Department of Polymer Science and Technology, Middle East Technical University, Ankara, 06800, Turkey
[c] Technical Sciences Vocational School, Gazi University, Ankara, 06500, Turkey
[d] Department of Chemistry, Middle East Technical University, Ankara, 06800, Turkey
[e] Department of Biotechnology, Middle East Technical University, Ankara, 06800, Turkey
[f] The Center for Solar Energy Research and Application (GUNAM), Middle East Technical University, Ankara, 06800, Turkey
[g] Centre of Excellence for Advanced Materials Research (CEAMR) and Chemistry Dept., Faculty of Science, King Abdulaziz University, P.O. Box 80203, Jeddah, 21589, Saudi Arabia

ARTICLE INFO

*Keywords:*
Conjugated molecules
Onium salts
Near-infrared sensitization
Photo-induced electron transfer
Radical polymerization
Cationic polymerization

ABSTRACT

In this communication, we report highly conjugated thiophenes having [1,2,5]-thiadiazolo and [1,2,5]-selenadiazolo [3,4-*f*]-benzo [1,2,3] triazole in conjunction with diphenyliodonium hexafluorophosphate salt (DPI) as new visible and near-infrared light (NIR) photoinitiator systems for free radical (FRP) and cationic polymerizations (CP). The postulated mechanism is based on the electron transfer reactions between the excited conjugated molecule and DPI ions. The radicals and Bronsted acid formed this way initiate FRP and CP of appropriate monomers such as methylacrylate (MA), methyl methacrylate (MMA), triethylene glycol dimethacrylate (TEGDMA) and cyclohexene oxide (CHO), isobutyl vinylether (IBVE) respectively. The possibility of *in situ* hybrid polymerization is also demonstrated using bifunctional monomer glycidyl methacrylate (GMA).

## 1. Introduction

Light-induced radical and cationic polymerization reactions have received considerable interest due to their advantages over traditional polymerization methods in terms of less energy consumption [1,2] (lower reaction temperature), reduced solvent use (greener) [3,4] and higher efficiency (faster reaction rates) [5–7]. These numerous advantages have led advances in the development of many photopolymerization products such as coatings [8], adhesives [9], nanomaterials [10], electronics [11], 3-D printings [12], artificial organs [13] and dental filling materials [14,15]. Most of the publications concerning photopolymerization reactions have focused on radical polymerization (FRP) methods. However, especially in the last two decades, scientists have put a great effort to obtain new interpenetrating polymer networks which can be formed by irradiating monomers possessing radically and cationically polymerizable functional units in the presence of appropriate photoinitiators (PIs) [16–18]. Onium salt type PIs can directly form hybrid cross-linked systems when the formulations are exposed to UV light. The most prominent onium salts are iodonium salts with large, non-nucleophilic counter anions, e.g. diphenyl iodonium salts (DPI). These salts when irradiated at the appropriate wavelength can readily undergo photochemical decomposition leading to the production of active species which can initiate both radical and cationic polymerizations [19]. The major drawback of DPI salts is related to their spectral sensitivity in UVB region (below 300 nm) which is a major health concern since UVB is harmful to living organisms and can damage eyes [20], industrially an important disadvantage [21]. The spectral sensitivity of DPI can be extended to visible range by the use of free radical photoinitiators [22] and photosensitizers (PS) [23,24]. Crivello and coworkers showed that polycyclic aromatic hydrocarbons (PAHs) such as pyrene can effectively be used for the photosensitization of aryliodonium salts in the visible light region according to the mechanism presented in Scheme 1 [25].

In our group, we showed that highly conjugated thiophene

* Corresponding author at: Department of Chemistry, Istanbul Technical University, Maslak, Istanbul, 34469, Turkey.
** Corresponding author at: Department of Polymer Science and Technology, Middle East Technical University, Ankara, 06800, Turkey.
*E-mail address:* yusuf@itu.edu.tr (Y. Yagci).

https://doi.org/10.1016/j.porgcoat.2021.106189
Received 20 November 2020; Received in revised form 31 January 2021; Accepted 3 February 2021
Available online 15 February 2021

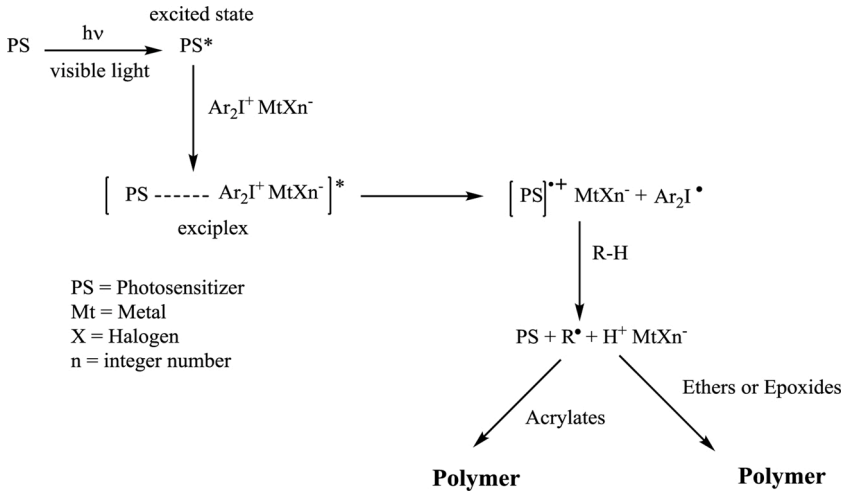


**Scheme 1.** PAH photosensitized radical and cationic polymerization mechanism of aryliodonium salts.

derivatives can also undergo similar photoinduced electron transfer reactions to generate radicalic and cationic species under visible light irradiation [26].

While many photoinitiators active in the visible range have been developed, photopolymerizations under NIR excitation are very limited [27]. The main advantages of NIR light over visible light include lower energy requirement [28], deeper penetration ability into materials which is crucial in photocuring applications [29] and heat release further favoring the polymerization process [30].

Photopolymerization reactions at NIR region are mostly achieved either by using NIR light absorbing dyes with electron donor properties that can undergo efficient photoelectron transfer reactions (PET) with OS (e.g. cyanine/OS couples) [28,31,32] or upconverting nanoparticles (UCNP) that absorb NIR light and upconvert it to higher energy near UV light which can activate different PIs [33,34].

On the other hand, thermal loss of light energy [35,42] and requirement of expensive laser systems emitting intense light [43] limit UCNPs wider usage in NIR induced polymerization applications.

Most of the NIR-sensitized polymerizations are based on photoinduced electron transfer (PET) reactions. In such systems, the related PET reactions seem to be different compare to that of the visible light system. Although the electron transfer entropy ($\Delta G_{et}$) using Rehm-Weller equation (Eq. (1)) between PI and various PS based on the oxidation potential ($E_{ox}$), active excitation energy E*(PS) of the photosensitizer and the reduction potential ($E_{red}$) of the PI are in the favorable negative range (0.5 V energy gap is sufficient) [36], no polymerization occurred under ambient infrared light [37].

$$\Delta G_{et} = E_{ox}\,(PS) - E_{red}\,(PI) - E^*(PS) \quad (1)$$

Strehmel and coworkers pointed out an internal activation barrier resulting in a system having a certain energy threshold and reaction temperature emphasizing the need of high intensity light source to overcome the internal energy barrier for most of the PET reactions (Equation 2) [38].

$$k_{et} = \nu.\kappa \times \exp(-\Delta G_{et}/RT) \quad (2)$$

where $\nu$ is theoretical maximal available rate and $\kappa$ is probability coefficient

In the light of this background, we herein report a new highly conjugated visible and NIR light photoiniating systems based on thiophene substituted [1,2,5]-thiadiazolo and [1,2,5]-selenadiazolo [3,4-*f*]-benzo [1,2,3] triazole, respectively in combination with diphenyliodonium hexafluorophosphate (DPI) for radical and cationic polymerizations of various monomers using a cheap incandescent light source. As will be shown below, the described system is also applicable to the hybrid polymerizations where both radical and cationic polymerizations proceed concomitantly.

## 2. Experimental

### 2.1. Materials

Diphenyliodonium hexafluorophosphate (DPI) >98 % was purchased from Sigma-Aldrich and was used without further purification. All the solvents and monomers were purified according to conventional purification methods prior to use. Photosensitizers 1a-b were synthesized with the yields of 41 % and 84 % respectively using the procedures as previously reported.

### 2.2. Photopolymerization procedure

A Philips 150 W PAR38E E27 halogen pressed glass type bulb with strong IR-A (NIR) emission (Fig. S1) was used for the photopolymerization reactions. The light intensity inside the reaction tube was calculated to be ~200 mW.cm$^{-2}$. The light bulb was attached to the top of a photoreactor setup equipped with a large air cooling fan and the reaction temperature was kept constant at room temperature. (24−25 °C). 25 mg of DPI (~0.06 mmol), 6.5 mg of PS (~0.01 mmol) and 1 mL of monofuncitonal and 2 mL of difunctional monomers (0.1−0.2 mmol) were dissolved in 1 mL of dichloromethane (DCM) and were transferred inside a 20 mL Schlenk tube which was previously heated, degassed and flushed with nitrogen for three times. After 2 h of irradiation (except for GMA which was irradiated for 24 h) inside the photoreactor, the polymers formed were precipitated into methanol. Obtained polymers were all colorful (Fig. S2) and were washed with hot methanol to remove of the unreacted PS. After washing procedure, the polymers were kept at least 24 h inside a vacuum-oven at 50 °C in order to avoid any solvent impurities. The conversions were determined by $^1$H-NMR analysis (Fig. S3).

### 2.3. Instruments

Obtained polymers were characterized using Gel Permeation Chromatography (GPC), infrared (IR), Nuclear Magnetic Resonance (NMR), ultraviolet-visible light (UV–vis) and fluorescence spectroscopies. Monomer conversions were determined gravimetrically. The PS trapped inside the polymers were identified by $^1$H-NMR Spectroscopy and subtracted from the gravimetric calculations using integral areas for accurate conversion calculations. Number average molecular weight ($M_n$) and dispersity indices ($Đ$) were determined using GPC with polystyrene

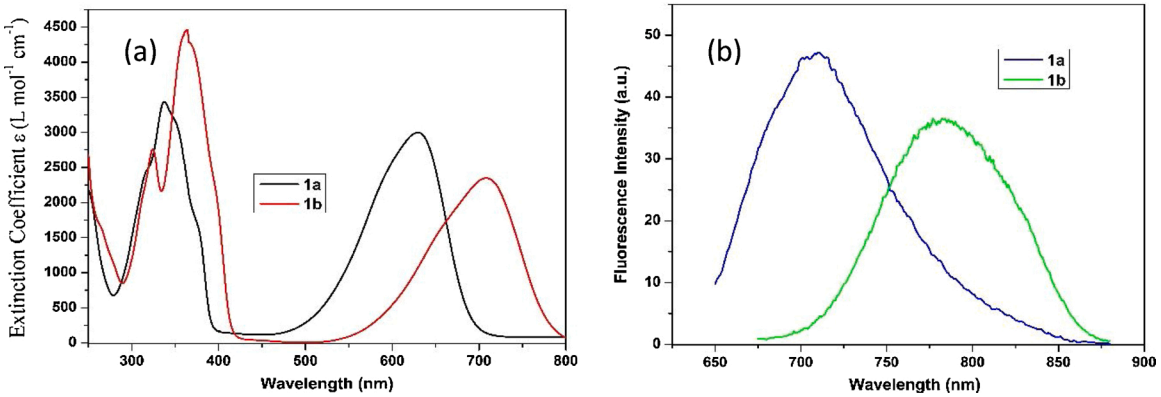


**Fig. 1.** (a) Optical absorption spectra of $3 \times 10^{-5}$ M dichloromethane solution of 1a (black) and 1b (red) (b) fluorescence spectra of $3 \times 10^{-8}$ M dichloromethane solution of 1a (blue) and 1b (green) excited at 600 nm and 655 nm, respectively. (For interpretation of the references to colour in this figure legend, the reader is referred to the web version of this article).

standards having very narrow molecular weight distribution. UV–vis spectra were recorded with a Shimadzu UV1601 double-beam spectrometer equipped with a 50 W halogen lamp and a deuterium lamp which can operate between 200–1100 nm. Fluorescence measurements were recorded on Perkin-Elmer LS55 instrument having a pulsed Xenon source. The slit widths were fixed to 10 nm. Measurement speeds were kept at 250 nm/min. Fourier-transform infrared (FTIR) spectra were recorded on Perkin–Elmer Spectrum One spectrometer with an ATR Accessory (ZnSe, Pike Miracle Accessory) and mercury cadmium telluride (MCT) detector. Sixteen scans were averaged. $^{1}$H-NMR (500 MHz) spectra were recorded in deuterated chloroform with tetramethylsilane as an internal standard on Agilent VNMRS500 spectrometer at 25 °C. Molecular weight measurements were conducted on a TOSOH EcoGPC system equipped with an auto sampler system, a temperature controlled pump, a column oven, a refractive index (RI) detector, a purge and degasser unit, and TSK gel superhZ2000 column with 4. 6 mm ID ×2 cm column dimensions. Tetrahydrofuran (THF) was used as the eluent at flow rate of 1.0 mL.min$^{-1}$ at 40 °C. RI detector was calibrated with polystyrene standards having very narrow molecular-weight distributions. GPC data were analyzed using Eco-GPC Analysis software. The electrochemical properties of the photosensitizers 1a and 1b were investigated via cyclic voltammetry (CV) in a solution of 0.1 M $Bu_4N^+PF_6^-$/DCM/ACN electrolyte/solvent couple at a scan rate of 100 mV/s. CV studies were performed in a three-electrode cell system by using ITO-coated glass as working electrode and platinum and silver wires as the counter and reference electrodes, respectively. (Fig. S4; Oxidation potentials for 1 a and 1 b are +1.06 V and +0.94 V). Dynamic mechanical analyses were performed using 15 mm of polymer films on a Perkin–Elmer Pyris Diamond DMA device working with a maximum force of 5 N between 10 °C–200 °C with 4 °C min$^{-1}$ temperature increase.

## 3. Results and discussion

As visible and NIR light sensitizers, newly designed conjugated molecules, 1a and 1b exhibit strong, broad absorbance with maxima at 620 nm and 710 nm (Fig. 1a), respectively and fluorescence emission in NIR region (Fig. 1b). The emission spectra of dichloromethane solutions of 1a and 1b gave perfect mirror-images of the absorbances with maxima at 725 nm and 800 mm when excited at 600 nm and 655 nm, respectively with appreciable Stokes shifts around 90 nm corresponding to IR-A region of the electromagnetic spectrum.

Considering the electron donating thiophene units present in the structures of 1a and 1b and their relevant oxidation potentials (Fig. S4), it is expected that the reactive species may be generated by PET. These reactions are well-known to cause variations in the fluorescence emissions leading to quenching [39,40]. Fluorescence quenching experiments were performed by exciting 1a and 1b using increasing amount of DPI (Fig. 2a–b). The results showed a sharp decrease upon addition of DPI to the solution of 1a. However, the change in the emission spectrum of 1b was much smaller suggesting a less efficient PET compared to that of 1a. This may be due to the larger atomic radius of selenium atom in 1b causing steric hindrance and limitation for an efficient PET reaction. The calculated plots (Fig. S5a–b) suggest dynamic quenching for both

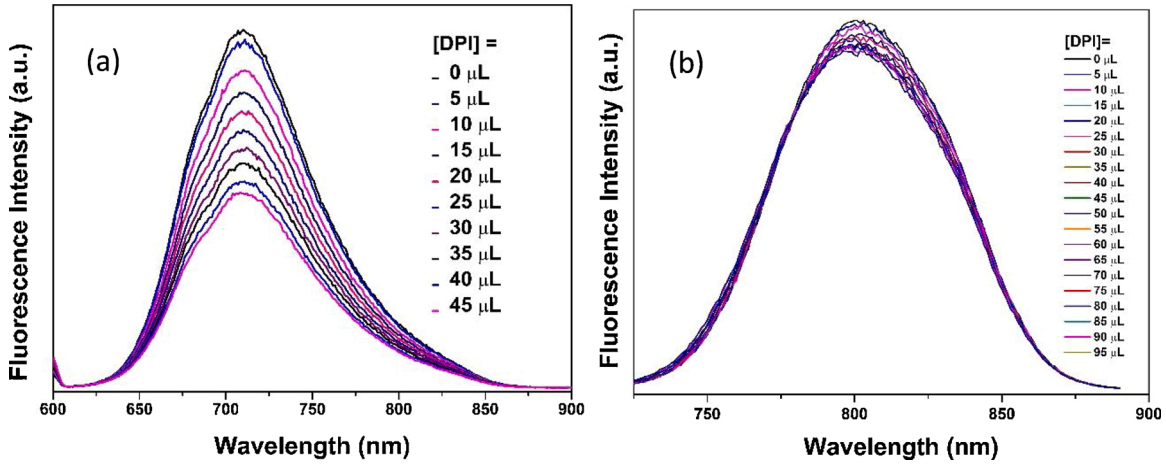


**Fig. 2.** Fluorescence spectra of 3 mL of (a) 1a excited at 600 nm and (b) 1b excited at 655 nm upon addition of 50 mM × 5μL DPI ($Ph_2I^+$ $PF_6^-$) in dichloromethane.

**Table 1**
NIR induced photopolymerization of various monomers by using 1a and 1b in the presence of $Ph_2I^+PF_6^-$.

| | Monomer [a] | Conversion [b] (%) | $M_n$ [c] (kg mol$^{-1}$) | $Đ$ [c] |
|---|---|---|---|---|
| 1a | CHO | 82.6 | 6.4 | 1.6 |
| 1a | IBVE | 92.0 | 84.0 | 1.7 |
| 1a | MMA | 8.2 | 56.5 | 1.6 |
| 1a | TEGDMA | 75.3 | nd | – |
| 1a | MA | 26.2 | 4.5 | 3.1 |
| 1a | GMA[d] | 92.2 | nd | – |
| 1b | CHO | 79.5 | 4.9 | 1.7 |
| 1b | IBVE | 69.6 | 96.8 | 1.5 |
| 1b | MMA | 1.6 | 48.5 | 1.8 |
| 1b | TEGDMA | 1.0 | nd | – |
| 1b | MA | 5.0 | 73.7 | 1.5 |
| 1b | GMA[d] | 90.8 | nd | – |

[a] Reaction conditions: 1 mL of dichloromethane, [monomer] ~ 1 × 10° M, [DPI] = 3 × 10$^{-2}$ M, [PS] = 5 × 10$^{-3}$ M, nominal wavelength = 700–1400 nm, t = 2 h, T = 25 °C.

[b] Precipitated in methanol and dried in vacuum oven, determined gravimetrically.

[c] Number average molecular weight (*Mn*) and dispersity (*Đ*) indices were determined using GPC (Gel Permeation Chromatography) according to polystyrene standards having very narrow molecular weight distribution.

[d] Reaction time was extended to 24 h. Abbreviation: nd, not determined.

compounds by DPI [41].

To examine the photosensitization activity of 1a and 1b for the iodonium salt under NIR irradiation, photopolymerizations of radical and cationically polymerizable monomers were conducted. Images of the resulting polymers given in the supporting information. (Fig. S6). Table 1 gives data for a series of polymerizations of various monomers utilizing 1a and 1b as NIR sensitizers and $Ph_2I^+PF_6^-$ as oxidant.

In analogous to the general photosensitization action of the conjugated thiophene derivatives, the electron transfer mechanism presented in Scheme 2 can be proposed.

Accordingly, upon NIR irradiation, electron transfer reactions result in the formation radical cation of photosensitizer ($PS^{+\cdot}$) and diphenyl iodo radical ($Ph_2I\cdot$). Bronsted acid released from the $PS^{\cdot+}$ is responsible for the initiation of the cationic polymerization. Direct initiation by $PS^{:+}$ can be discarded since the transients of structurally similar thiophene derivatives were not efficiently quenched by epoxy monomers [42]. The concomitantly formed $Ph_2I\cdot$ radical rapidly decomposes to the iodobenzene and phenyl radical capable of initiating radical polymerization.

As can be seen from Table 1 both PSs have lower initiation efficiency for radical polymerization compare to the corresponding cationic mode. This may be explained by the coupling reactions of propagating radicals with $PS^{\cdot+}$ accompanied by the proton release (Scheme 3). This behavior was further evidenced by the spectral characterization of the polymers thus formed (vide infra) (Fig. 3). Notably, 1a appears to be more efficient in initiation of both polymerizations. Although 1b has thermodynamically more favorable redox potential for the electron transfer reaction, the observed lower efficiency can be attributed to the lower

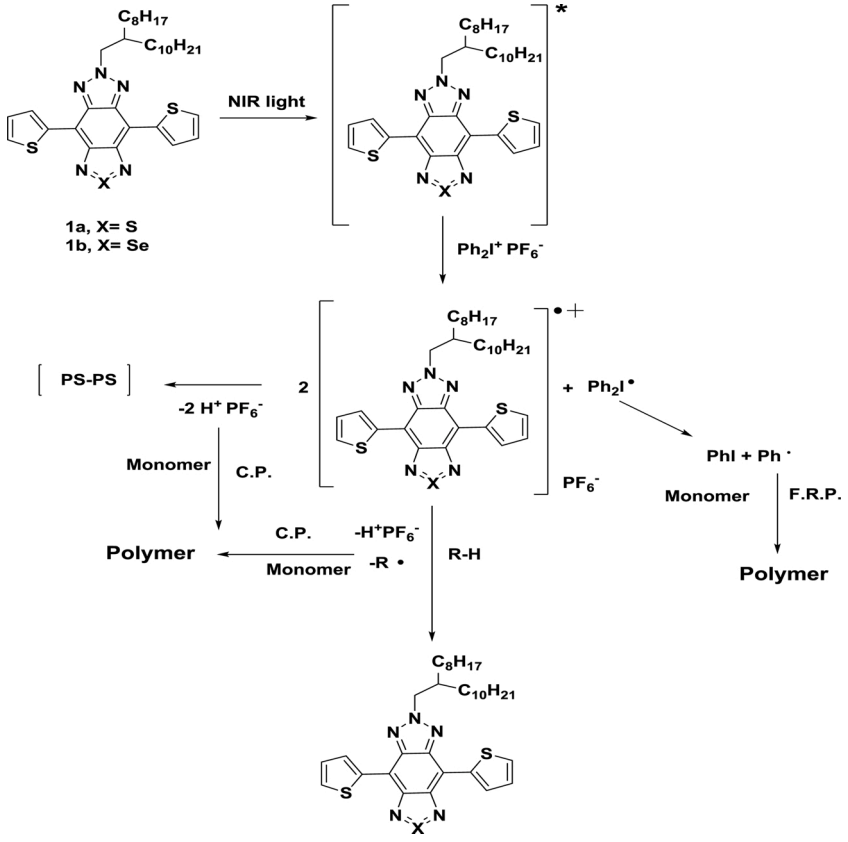


**Scheme 2.** Proposed reaction mechanisms with different pathways for NIR-sensitized polymerization.

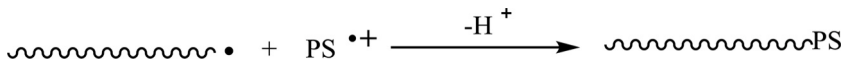


**Scheme 3.** Coupling reaction of propagating radicals with photosensitizer radical cation.

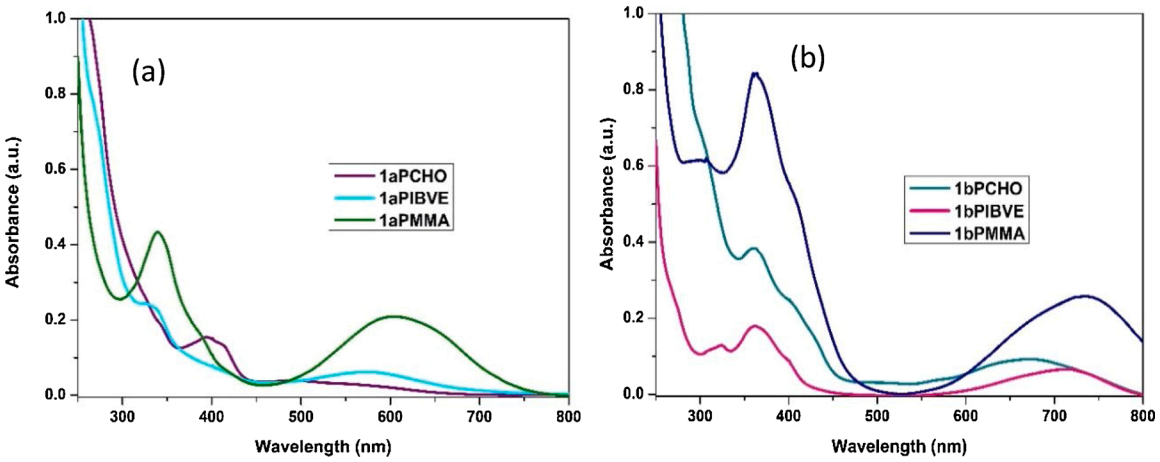


**Fig. 3.** UV absorbance of the polymers obtained using (a) 1a and (b) 1b.

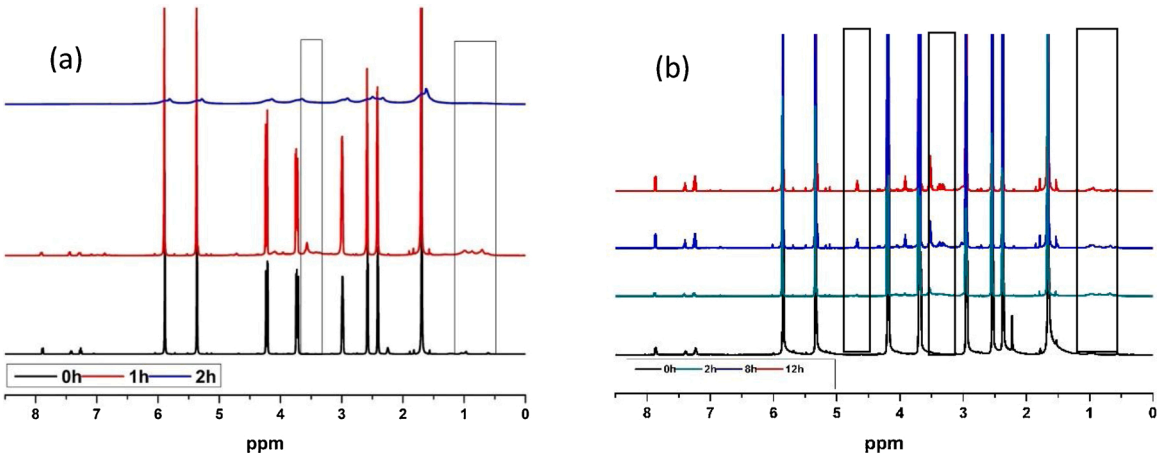


**Fig. 4.** $^{1}$H-NMR spectra changes over time of GMA after NIR irradiation (a) using 1a and (b) using 1b in $CDCl_3$ (500 MHz).

absorbance and higher atomic radius of selenium heteroatom in the structure. The higher conversions were attained with a highly reactive, electron donor monomer, IBVE. Besides initiation by Bronsted acids, the electron donating radicals formed by the addition of the radicals can be oxidized to the corresponding carbocations. Thus, polymerization proceeds through both initiation routes.

Fig. 3a–b show absorbance spectra of the polymers obtained. As can be seen, PMMA has stronger absorbance in the region where the photosensitizers absorb indicating possible coupling reactions coupling reactions of the sensitizer derived radicals with the propagating radicals.

Experiments were also performed using glycidyl methacrylate (GMA) as hybrid monomer having both radical and cationically polymerizable functions. Real-time $^{1}$H-NMR measurements were performed to investigate the efficiency of sensitizers at the same amount of DPI and monomer in the NMR tube. Results showed the higher efficiency of 1a over 1b in agreement with the Stern-Volmer quenching experiments and gravimetric conversions (Fig. 4a–b). For the photopolymerization of GMA using 1a, 1 h of NIR irradiation showed new peaks corresponding to new methyl groups (acrylate methyl) around 1 ppm and changes in $-CH_2$ protons attached to oxirane unit. After 2 h of irradiation a complete gelation occurred which gave broad peaks due to cross-linking. Notably, the spectral changes and gelation were relatively slower with 1b.

Due to the fact that the networks formed by the hybrid monomer GMA are highly brittle [43], dynamic mechanical analysis (DMA) was performed using a hybrid system consisitng of TEGDMA / poly(propylene glycol) diglycidyl ether ($M_n$~380) mixtures in the presence of 1a. The films formed by polymerization of this mixture (Fig. S7) using 1a under both UV (~350 nm) and NIR light showed different glass transition temperatures (Fig. S8). The maximum of the tanD curve signalizes the glass transition temperature of the film obtained. It depicts one glass transition temperature appearing at ~60 °C for the UV-system and at ~120 °C for the NIR-system demonstrating the superiority of the NIR light over UV light due to the heat release.

## 4. Conclusion

In conclusion, highly conjugated thiophene molecules with sulfur and selenium hetero atoms as visible and NIR light photosensitizers for both radical and cationic polymerizations were reported for the first time. The initiation is based on the PET reactions occurred between the photosensitizer and DPI. The radicals and cationic species thus formed are responsible for the initiation of the respective polymerization. The cationic mode appeared to be more efficient due to the possible coupling reactions of the radical process. Potential application of the initiating system for dual polymerization was demonstrated by using a bifunctional monomer possessing both radical and cationic polymerizable groups. Further studies are in progress to adapt the described photoinitiating system to step-growth polymerization.

## CRediT authorship contribution statement

**Ali Suerkan:** Data curation, Formal analysis. **Ecem Aydan Alkan:** . **Kerem Kaya:** Writing - original draft, Validation, Investigation.

**Yasemin Arslan Udum:** Investigation. **Levent Toppare:** Supervision. **Yusuf Yagci:** Supervision, Writing - review & editing.

## Declaration of Competing Interest

The authors declare no competing interest.

## Acknowledgements

This work was supported by Istanbul Technical University Research Fund.

## Appendix A. Supplementary data

Supplementary material related to this article can be found, in the online version, at doi:https://doi.org/10.1016/j.porgcoat.2021.106189.

## References

[1] S. Dadashi-Silab, S. Doran, Y. Yagci, Photoinduced electron transfer reactions for macromolecular syntheses, Chem. Rev. 116 (17) (2016) 10212–10275.
[2] J.P. Fouassier, X. Allonas, D. Burget, Photopolymerization reactions under visible lights: principle, mechanisms and examples of applications, Prog. Org. Coat. 47 (1) (2003) 16–36.
[3] M.A. Dubé, S. Salehpour, Applying the principles of green chemistry to polymer production technology, Macromol. React. Eng. 8 (1) (2014) 7–28.
[4] Photoinitiators for Free radical polymerization reactions, Photochem. Photophys. Polym. Mater. (2010) 351–419.
[5] E. Andrzejewska, Photopolymerization kinetics of multifunctional monomers, Prog. Polym. Sci. 26 (4) (2001) 605–665.
[6] Y. Yagci, S. Jockusch, N.J. Turro, Photoinitiated polymerization: advances, challenges, and opportunities, Macromolecules 43 (15) (2010) 6245–6260.
[7] M. Sangermano, I. Roppolo, A. Chiappone, New horizons in cationic photopolymerization, Polymers 10 (2) (2018) 136.
[8] C. Mendes-Felipe, J. Oliveira, I. Etxebarria, J.L. Vilas-Vilela, S. Lanceros-Mendez, State-of-the-art and future challenges of UV curable polymer-based smart materials for printing technologies, Adv. Mater. Technol. 4 (3) (2019), 1800618.
[9] H. Gong, X. Guo, D. Cao, P. Gao, D. Feng, X. Zhang, Z. Shi, Y. Zhang, S. Zhu, Z. Cui, Photopolymerizable and moisture-curable polyurethanes for dental adhesive applications to increase restoration durability, J. Mater. Chem. B 7 (5) (2019) 744–754.
[10] A. Medellin, W. Du, G. Miao, J. Zou, Z. Pei, C. Ma, Vat photopolymerization 3D printing of nanocomposites: a literature review, J. Micro Nano-manufacturing 7 (3) (2019).
[11] M. Layani, X. Wang, S. Magdassi, Novel materials for 3D printing by photopolymerization, Adv. Mater. 30 (41) (2018), 1706344.
[12] A. Bagheri, J. Jin, Photopolymerization in 3D printing, ACS Appl. Polymer Mater. 1 (4) (2019) 593–611.
[13] B. Baroli, Photopolymerization of biomaterials: issues and potentialities in drug delivery, tissue engineering, and cell encapsulation applications, J. Chem. Technol. Biotechnol. 81 (4) (2006) 491–499.
[14] J.W. Stansbury, Curing dental resins and composites by photopolymerization, J. Esthet. Restor. Dent. 12 (6) (2000) 300–308.
[15] M. Topa, J. Ortyl, Moving towards a finer way of light-cured resin-based restorative dental materials: recent advances in photoinitiating systems based on iodonium salts, Materials 13 (18) (2020) 4093.
[16] J. Shao, Y. Huang, Q. Fan, Visible light initiating systems for photopolymerization: status, development and challenges, Polym. Chem. 5 (14) (2014) 4195–4210.
[17] S. Shi, F. Karasu, C. Rocco, X. Allonas, C. Croutxé-Barghorn, Photoinitiating systems for LED-Cured interpenetrating polymer networks, J. Photopolym. Sci. Technol. 28 (2015) 31–35.
[18] J. Ortyl, P. Fiedor, A. Chachaj-Brekiesz, M. Pilch, E. Hola, M. Galek, The applicability of 2-amino-4,6-diphenyl-pyridine-3-carbonitrile sensors for monitoring different types of photopolymerization processes and acceleration of cationic and free-radical photopolymerization under near UV light, Sensors (Basel) 19 (7) (2019) 1668.
[19] J.V. Crivello, J.H.W. Lam, Diaryliodonium salts. A new class of photoinitiators for cationic polymerization, Macromolecules 10 (6) (1977) 1307–1315.
[20] B. Aydogan Temel, B. Gacal, A. Yildirim, N. Yonet, Y. Yuksel, Y. Yagci, Wavelength tunability in photoinitiated cationic polymerization. Photochemistry and UV Curing: New Trends, 2006.
[21] J.-P. Fouassier, Photoinitiation, Photopolymerization, and Photocuring: Fundamentals and Applications, Hanser, 1995.
[22] K. Kaya, M. Seba, T. Fujita, S. Yamago, Y. Yagci, Visible light-induced free radical promoted cationic polymerization using organotellurium compounds, Polym. Chem. 9 (48) (2018) 5639–5643.
[23] K. Kostrzewska, J. Ortyl, R. Dobosz, J. Kabatc, Squarylium dye and onium salts as highly sensitive photoradical generators for blue light, Polym. Chem. 8 (2017) 3464–3474.
[24] J. Kabatc, J. Ortyl, K. Kostrzewska, New kinetic and mechanistic aspects of photosensitization of iodonium salts in photopolymerization of acrylates, RSC Adv. 7 (66) (2017) 41619–41629.
[25] J.V. Crivello, F. Jiang, Development of pyrene photosensitizers for cationic photopolymerizations, Chem. Mater. 14 (11) (2002) 4858–4866.
[26] S. Beyazit, B. Aydogan, I. Osken, T. Ozturk, Y. Yagci, Long wavelength photoinitiated free radical polymerization using conjugated thiophene derivatives in the presence of onium salts, Polym. Chem. 2 (5) (2011) 1185–1189.
[27] B. Strehmel, C. Schmitz, T. Bromme, A. Halbhuber, D. Oprych, J.S. Gutmann, Advances of near infrared sensitized radical and cationic photopolymerization: from graphic industry to traditional coatings, J. Photopolym. Sci. Technol. 29 (1) (2016) 111–121.
[28] A.H. Bonardi, F. Dumur, T.M. Grant, G. Noirbent, D. Gigmes, B.H. Lessard, J. P. Fouassier, J. Lalevée, High performance near-infrared (NIR) photoinitiating systems operating under low light intensity and in the presence of oxygen, Macromolecules 51 (4) (2018) 1314–1324.
[29] R. Liu, X. Zou, Y. Xu, X. Liu, Z. Li, Deep thiol-ene photopolymerization using upconversion nanoparticle-assisted photochemistry, Chem. Lett. 45 (9) (2016) 1054–1056.
[30] C. Schmitz, D. Oprych, C. Kutahya, B. Strehmel, Chapter 14 NIR light for initiation of photopolymerization. In Photopolymerisation Initiating Systems, The Royal Society of Chemistry, 2018, pp. 431–478.
[31] T. Brömme, D. Oprych, J. Horst, P. Pinto, B. Strehmel, New iodonium salts in NIR sensitized radical photopolymerization of multifunctional monomers, RSC Adv. 5 (2015).
[32] J. Kabatc, K. Iwińska, A. Balcerak, D. Kwiatkowska, A. Skotnicka, Z. Czech, M. Bartkowiak, Onium salts improve the kinetics of photopolymerization of acrylate activated with visible light, RSC Adv. 10 (42) (2020) 24817–24829.
[33] X. Meng, H. Lu, Z. Li, C. Wang, R. Liu, X. Guan, Y. Yagci, Near-infrared light induced cationic polymerization based on upconversion and ferrocenium photochemistry, Polym. Chem. 10 (41) (2019) 5574–5577.
[34] A. Kocaarslan, S. Tabanli, G. Eryurek, Y. Yagci, Near-infrared free-radical and free-radical-promoted cationic photopolymerizations by in-source lighting using upconverting glass, Angew. Chemie Int. Ed. 56 (46) (2017) 14507–14510.
[35] B.D. Ravetz, N.E.S. Tay, C.L. Joe, M. Sezen-Edmonds, M.A. Schmidt, Y. Tan, J. M. Janey, M.D. Eastgate, T. Rovis, Development of a platform for near-infrared photoredox catalysis, ACS Cent. Sci. (2020).
[36] E. Hola, M. Pilch, M. Galek, J. Ortyl, New versatile bimolecular photoinitiating systems based on amino-m-terphenyl derivatives for cationic, free-radical and thiol–ene photopolymerization under low intensity UV-A and visible light sources, Polym. Chem. 11 (2) (2020) 480–495.
[37] C. Schmitz, A. Halbhuber, D. Keil, B. Strehmel, NIR-sensitized photoinitiated radical polymerization and proton generation with cyanines and LED arrays, Prog. Org. Coat. 100 (2016) 32–46.
[38] C. Schmitz, Y. Pang, A. Gülz, M. Gläser, J. Horst, M. Jäger, B. Strehmel, New high-power LEDs open photochemistry for near-infrared-Sensitized radical and cationic photopolymerization, Angew. Chemie Int. Ed. 58 (13) (2019) 4400–4404.
[39] S. Doose, H. Neuweiler, M. Sauer, Fluorescence quenching by photoinduced Electron transfer: a reporter for conformational dynamics of macromolecules, ChemPhysChem 10 (9–10) (2009) 1389–1398.
[40] M.H. Gehlen, The centenary of the Stern-Volmer equation of fluorescence quenching: from the single line plot to the SV quenching map, J. Photochem. Photobiol. C Photochem. Rev. 42 (2020), 100338.
[41] D.M. Arias-Rotondo, J.K. McCusker, The photophysics of photoredox catalysis: a roadmap for catalyst design, Chem. Soc. Rev. 45 (21) (2016) 5803–5820.
[42] Y. Yagci, S. Jockusch, N.J. Turro, Mechanism of photoinduced step polymerization of thiophene by onium salts: reactions of phenyliodinium and diphenylsulfinium radical cations with thiophene, Macromolecules 40 (13) (2007) 4481–4485.
[43] J.-t. Yeh, C.-h. Tsou, Y.-m. Li, H.-w. Xiao, C.-s. Wu, W.-l. Chai, Y.-C. Lai, C.-K. Wang, The compatible and mechanical properties of biodegradable poly(Lactic Acid)/ethylene glycidyl methacrylate copolymer blends, J. Polym. Res. 19 (2) (2012) 9766.